Biomedical Optics EXPRESS

Single camera imaging system for color and near-infrared fluorescence image guided surgery

Zhenyue Chen,[1,2] Nan Zhu,[1] Shaun Pacheco,[1] Xia Wang,[2] and Rongguang Liang [1,*]

[1] *College of Optical Sciences, University of Arizona, Tucson, Arizona 85721, USA*
[2]*Beijing Institute of Technology, Key Laboratory of Photoelectronic Imaging Technology and System of Ministry of Education of China, School of Optoelectronics, Beijing 100081, China*
** rliang@optics.arizona.edu*

Abstract: Near-infrared (NIR) fluorescence imaging systems have been developed for image guided surgery in recent years. However, current systems are typically bulky and work only when surgical light in the operating room (OR) is off. We propose a single camera imaging system that is capable of capturing NIR fluorescence and color images under normal surgical lighting illumination. Using a new RGB-NIR sensor and synchronized NIR excitation illumination, we have demonstrated that the system can acquire both color information and fluorescence signal with high sensitivity under normal surgical lighting illumination. The experimental results show that ICG sample with concentration of 0.13 μM can be detected when the excitation irradiance is 3.92 mW/cm^2 at an exposure time of 10 ms.

OCIS codes: (170.3890) Medical optics instrumentation; (110.0110) Imaging systems; (110.2970) Image detection systems; (300.2530) Fluorescence, laser-induced; (170.1610) Clinical applications; (100.2980) Image enhancement.

References and links

1. G. Themelis, J. S. Yoo, K. S. Soh, R. Schulz, and V. Ntziachristos, "Real-time intraoperative fluorescence imaging system using light-absorption correction," J. Biomed. Opt. **14**(6), 064012 (2009).
2. J. V. Frangioni, "In vivo near-infrared fluorescence imaging," Curr. Opin. Chem. Biol. **7**(5), 626–634 (2003).
3. G. M. van Dam, G. Themelis, L. M. Crane, N. J. Harlaar, R. G. Pleijhuis, W. Kelder, A. Sarantopoulos, J. S. de Jong, H. J. Arts, A. G. van der Zee, J. Bart, P. S. Low, and V. Ntziachristos, "Intraoperative tumor-specific fluorescence imaging in ovarian cancer by folate receptor-α targeting: first in-human results," Nat. Med. **17**(10), 1315–1319 (2011).
4. E. M. Sevick-Muraca, "Translation of near-infrared fluorescence imaging technologies: emerging clinical applications," Annu. Rev. Med. **63**(1), 217–231 (2012).
5. W. Stummer, U. Pichlmeier, T. Meinel, O. D. Wiestler, F. Zanella, and H. J. Reulen; ALA-Glioma Study Group, "Fluorescence-guided surgery with 5-aminolevulinic acid for resection of malignant glioma: a randomised controlled multicentre phase III trial," Lancet Oncol. **7**(5), 392–401 (2006).
6. V. Venugopal, M. Park, Y. Ashitate, F. Neacsu, F. Kettenring, J. V. Frangioni, S. P. Gangadharan, and S. Gioux, "Design and characterization of an optimized simultaneous color and near-infrared fluorescence rigid endoscopic imaging system," J. Biomed. Opt. **18**(12), 126018 (2013).
7. M. V. Marshall, J. C. Rasmussen, I. C. Tan, M. B. Aldrich, K. E. Adams, X. Wang, C. E. Fife, E. A. Maus, L. A. Smith, and E. M. Sevick-Muraca, "Near-infrared fluorescence imaging in humans with indocyanine green: a review and update," Open Surg Oncol J **2**(2), 12–25 (2010).
8. S. L. Troyan, V. Kianzad, S. L. Gibbs-Strauss, S. Gioux, A. Matsui, R. Oketokoun, L. Ngo, A. Khamene, F. Azar, and J. V. Frangioni, "The FLARE Intraoperative Near-Infrared Fluorescence Imaging System: A First-in-Human Clinical Trial in Breast Cancer Sentinel Lymph Node Mapping," Ann. Surg. Oncol. **16**(10), 2943–2952 (2009).
9. http://www.fluoptics.com/fluoptics_Fluorescence_Imaging_System.php
10. http://www.iht-ltd.com/pde-photodynamic-eye/
11. M. Takahashi, T. Ishikawa, K. Higashidani, and H. Katoh, "SPY: an innovative intra-operative imaging system to evaluate graft patency during off-pump coronary artery bypass grafting," Interact. Cardiovasc. Thorac. Surg. **3**(3), 479–483 (2004).
12. J. Lee and E. Sevick-Muraca, "Fluorescence-enhanced absorption imaging using frequency-domain photon migration: tolerance to measurement error," J. Biomed. Opt. **6**(1), 58–67 (2001).
13. K. Sexton, S. C. Davis, D. McClatchy 3rd, P. A. Valdes, S. C. Kanick, K. D. Paulsen, D. W. Roberts, and B. W. Pogue, "Pulsed-light imaging for fluorescence guided surgery under normal room lighting," Opt. Lett. **38**(17), 3249–3252 (2013).

#212401 - $15.00 USD Received 20 May 2014; revised 17 Jul 2014; accepted 19 Jul 2014; published 25 Jul 2014

14. T. Handa, R. G. Katare, S. Sasaguri, and T. Sato, "Preliminary experience for the evaluation of the intraoperative graft patency with real color charge-coupled device camera system: an advanced device for simultaneous capturing of color and near-infrared images during coronary artery bypass graft," Interact. Cardiovasc. Thorac. Surg. **9**(2), 150–154 (2009).
15. S. Keereweer, P. B. Van Driel, T. J. Snoeks, J. D. Kerrebijn, R. J. Baatenburg de Jong, A. L. Vahrmeijer, H. J. Sterenborg, and C. W. Löwik, "Optical image-guided cancer surgery: challenges and limitations," Clin. Cancer Res. **19**(14), 3745–3754 (2013).
16. B. Zhu, J. C. Rasmussen, and E. M. Sevick-Muraca, "Non-invasive fluorescence imaging under ambient light conditions using a modulated ICCD and laser diode," Biomed. Opt. Express **5**(2), 562–572 (2014).
17. Z. Chen, X. Wang, and R. Liang, "RGB-NIR multispectral camera," Opt. Express **22**(5), 4985–4994 (2014).
18. J. Glatz, J. Varga, P. B. Garcia-Allende, M. Koch, F. R. Greten, and V. Ntziachristos, "Concurrent video-rate color and near-infrared fluorescence laparoscopy," J. Biomed. Opt. **18**(10), 101302 (2013).

1. Introduction

Near-infrared (NIR) fluorescence imaging techniques have been developed for a number of clinical applications, ranging from improving tumor delineation, sentinel lymph node identification, and metastasis staging, to neuronal activity monitoring [1]. Because the fluorescence imaging can provide high sensitive and real-time information of the surgical fields, it is a very promising technique for image guided surgery (IGS) [2–5]. The fluorescence signal either arises from endogenous fluorophores or exogenous fluorophores, for instance, indocyanine green (ICG) and methylene blue (MB) [6, 7]. A number of fluorescence imaging systems using ICG or MB have been developed, such as FLARE imaging [8], fluobeam [9], Photodynamic Eye [10], SPY [11], FDPM imager [12], and so on. Most of imaging systems either used single image sensor to capture visible and fluorescence images sequentially or use multiple cameras to image different spectra simultaneously or sequentially [1, 6, 13]. One common issue of current fluorescence image guided surgical systems is that the surgical light has to be turned off or dimed significantly to improve fluorescence image contrast [1, 13–15]. To address this problem, Sexton et al. presented a fluorescence guided surgery system using pulsed excitation and gated acquisition [13]. This approach works well under the normal surgical lighting condition, it is relatively complicated because a fast filter wheel is needed to work with pulsed excitation. A number of spectral images are required to obtain the color information and fluorescent signal, resulting in a low imaging speed. Zhu et.al demonstrated far-red and NIR fluorescence imaging system using a modulated ICCD and laser diode operated in homodyne detection [16]. Three images with different phase delays are required to obtain the AC amplitude image and DC image.

In this paper, we propose a novel single camera color and NIR fluorescence imaging system that is capable of capturing color and fluorescence images under normal surgical lighting illumination, using a single RGB-NIR camera and synchronized excitation illumination.

2. Single camera color and NIR fluorescence imaging system

The proposed system is shown in Fig. 1. A new type of CMOS sensor with four color filter arrays (CFA) is used to capture color image and NIR fluorescence image. The frame rate is 60 fps with a resolution of 2304x1296 in 12 bit depth. This camera has four color channels (NIR, red, green, and blue), compared to 3 channels in conventional color camera. An external 2 W 785 nm diode laser with 4 nm spectral width is used to excite NIR fluorescence from ICG, it is synchronized to the camera. A 25 mm VIS-NIR compact fixed focal length lens from Edmund Optics is used to image the sample to the RGB-NIR sensor; this lens has good transmission in visible and NIR bands. A notch filter (Edmund Optics 86127) with a center wavelength of 785 nm and an FWHM bandwidth of 33 nm is placed in front of the camera lens to block the excitation light. With the synchronized NIR excitation illumination, the camera captures videos/images with and without excited NIR fluorescence under the normal surgical room lighting condition in real time. Four images, R, G, B, and NIR, are extracted from the corresponding channels in the raw image. The fluorescence signal is then extracted from the two NIR images captured with and without NIR excitation illumination. Compared to other systems addressing the normal lighting issue in OR, the proposed system

#212401 - $15.00 USD Received 20 May 2014; revised 17 Jul 2014; accepted 19 Jul 2014; published 25 Jul 2014

is very simple and compact without moving part, it has a high sensitivity in detecting NIR fluorescence signal. It can also capture color reflectance and NIR fluorescence images in real time; the color reflectance image and NIR fluorescence image are well-aligned because both of them are captured at the same time.

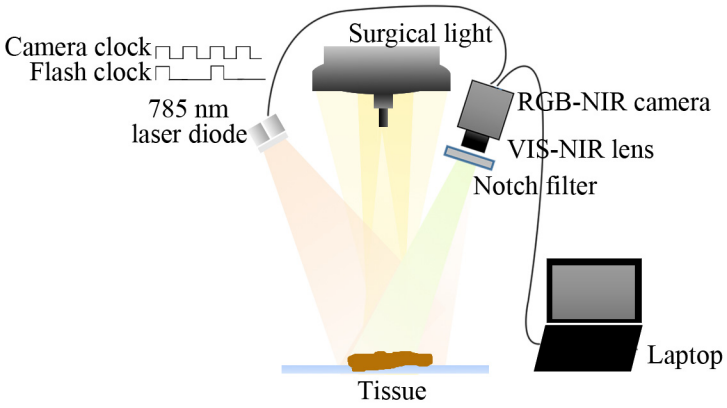

Fig. 1. Schematic diagram of the experimental setup.

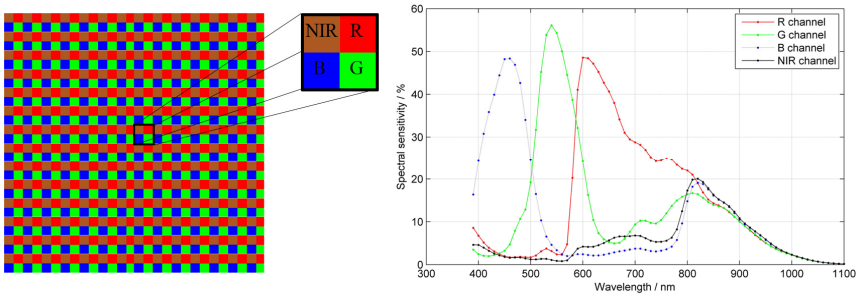

Fig. 2. (a) Color filter arrays with four bandpass filters in RGB-NIR camera and (b) spectral sensitivity of the color filter arrays [17].

Figure 2(a) is the layout of the new CFA, and Fig. 2(b) is the typical spectral sensitivity [17]. As shown in Fig. 2(b), there is cross-talks between the R, G, B, and NIR channels. The color image channels, i.e. R, G and B, are sensitive to NIR component. The NIR channel is also not ideal and is sensitive to visible light, but this is less significant. We have developed an image processing technique to extract accurate color image and NIR image from raw images. The four images of the standard X-Rite ColorChecker, R, G, B and NIR, are used as the calibration targets. Since the output RGB values from the camera and the destination values of the ColorChecker are known, a mapping color correction matrix (CCM) is estimated from these two group values and used to extract the R, G, B and NIR images from raw data [17]

3. System performance

To demonstrate the system concept and evaluate system performance, a set of ICG samples with various concentrations in dimethylsulfoxide (DMSO) were prepared. The ICG concentrations were 10.32 μM, 5.16 μM, 2.58 μM, 1.29 μM, 0.65 μM, 0.32 μM, 0.13 μM, and 0 μM respectively. The samples were placed directly under the CHROMOPHARE F generation surgical light. In our experiment, the power of the surgical light was measured approximately 45,000 lx. The spectra of the surgical light with normal fluorescent room light

#212401 - $15.00 USD Received 20 May 2014; revised 17 Jul 2014; accepted 19 Jul 2014; published 25 Jul 2014

on/off were measured with Ocean Optics HR2000 + spectrometer and are shown in Fig. 3, the two measurements are almost overlapped. The inset (a) is the NIR spectrum of the fluorescent light, it is the difference of NIR spectrum between the two measurements with the fluorescent room light on/off. From the measured spectra and the inset (a), it is clear that the impact of the fluorescent room light on NIR fluorescence imaging is negligible. The NIR spectrum of the LED surgical light (inset (b)) has significantly negative impact on NIR fluorescence imaging; it reduces the ICG fluorescence image contrast because it overlaps the ICG fluorescence. This impact should be minimized in clinical applications.

The 785 nm laser diode was driven by Tektronix PWS4205 linear DC power supplier. A Newport 1916-R hand-held optical power meter was employed to measure the excitation NIR light radiation at the surface of the sample. The irradiance around 785 nm at the surface of the sample was ~5.5 mW/cm^2

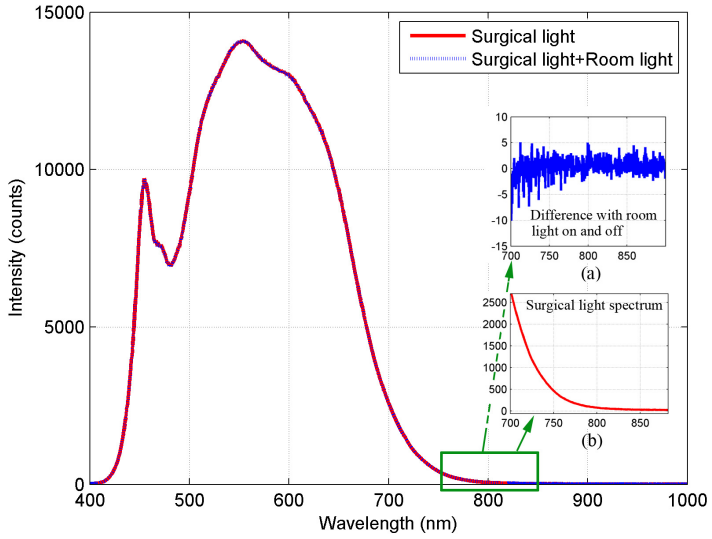

Fig. 3. Spectra of surgical light with the normal fluorescent room light on/off. The inset (a) is the NIR spectrum difference with the fluorescent room light on/off and the inset (b) is the NIR spectrum of the surgical light between 700 nm and 900 nm.

Figure 4(a) is the raw image of USAF 1951 test target when illuminated with white light and NIR light at 850 nm, Figs. 4(b) and 4(c) are images extracted from Green channel and NIR channel. Both extracted images can resolve 12.7 line pairs/mm, corresponding to the resolution of 78.7 μm in the object plane. Figures 5(a) and 5(b) are the NIR channel images extracted from the raw images captured when the NIR excitation laser was off and on under normal surgical lighting condition. The measurement was carried out with an integration time of 10 ms; the camera exposure time was restricted mainly by the surgical light. The bases of the ICG containers are bright because of the NIR components from the surgical light, the central ICG containers in Fig. 5(a) are brighter because the illumination from the surgical light is not uniform. Figure 5(b) is the NIR fluorescence images of ICG samples with the excitation light on, no fluorescence signal is detected from pure DMSO (the right container with 0 μM ICG concentration). It is also clear from Fig. 5(c) which is the difference image between Fig. 5(a) and Fig. 5(b), the background information is removed and fluorescence information is highlighted.

#212401 - $15.00 USD Received 20 May 2014; revised 17 Jul 2014; accepted 19 Jul 2014; published 25 Jul 2014

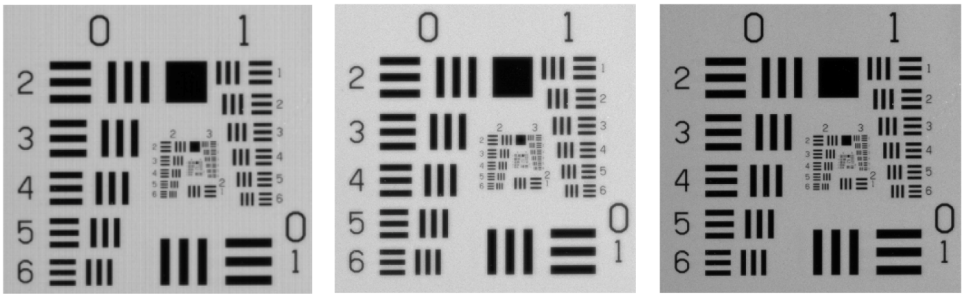

(a) (b) (c)

Fig. 4. Raw and extracted images of the USAF 1951 test target under visible and NIR (850 nm) illumination. (a) Raw image, (b) image extracted from Green channel, and (c) image extracted from NIR channel

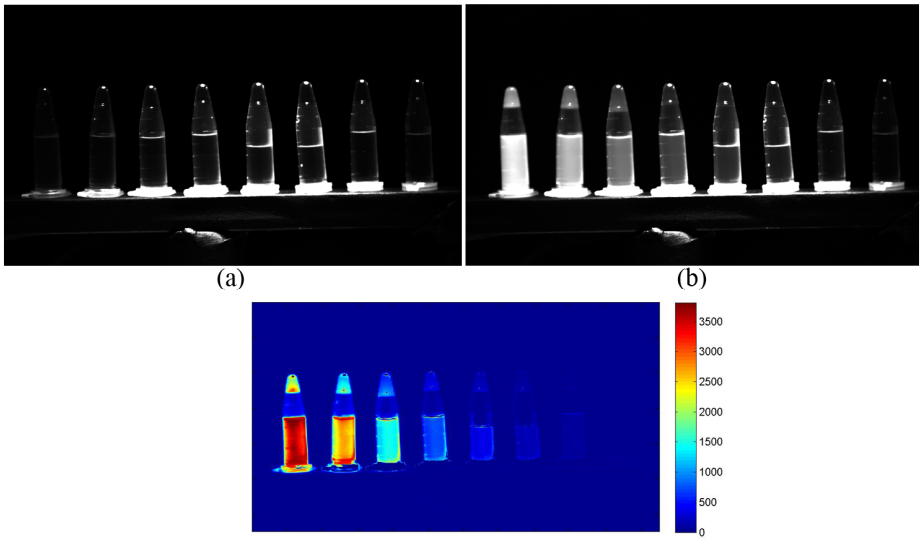

(a) (b)

(c)

Fig. 5. (a) NIR image of ICG samples under normal surgical lighting condition; (b) NIR image of ICG samples under the surgical lighting condition with excitation light on; (c) Difference image between (a) and (b). The concentration of ICG from left to right are 10.32 μM, 5.16 μM, 2.58 μM, 1.29 μM, 0.65 μM, 0.32 μM, 0.13 μM and 0 μM respectively.

A 50x50 pixels region of interest (ROI) is set at the center of each sample in Fig. 5(c) to count the pixel values. The bit depth of the sensor is 12-bit, so the maximum gray level is 4095. The sensitivity curves of the system are shown in Fig. 6(a). It can be seen that, with stronger excitation irradiance, fluorescence signal is stronger. Here, we set the sample with ICG concentration of 0 μM (pure DMSO) as background. Figure 6(a) shows the fluorescence signal intensity which is represented by the mean pixel value of each ROI. Figure 6(b) shows the signal-to-noise ratio (SNR) in dB versus ICG concentration and NIR excitation power. The SNR is calculated as [18]

$$SNR_{dB} = 20\log_{10}(\frac{S}{RMSN}), \quad (1)$$

where S is the mean signal intensity and $RMSN$ is the root-mean-square noise within the ROI.

For a normal signal distribution a confidence level of 99.7% corresponds to 9.5 dB on the dB scale [18]. Thus from Fig. 6(b), it is clear that the sample with concentration of 0.32 μM

#212401 - $15.00 USD Received 20 May 2014; revised 17 Jul 2014; accepted 19 Jul 2014; published 25 Jul 2014

can be detected confidently when the excitation irradiance reaches 2.62 mW/cm^2 with the exposure time of 10 ms; the sample with concentration of 0.13 μM can be detected when the irradiance is stronger than 3.92 mW/cm^2 with the exposure time of 10 ms.

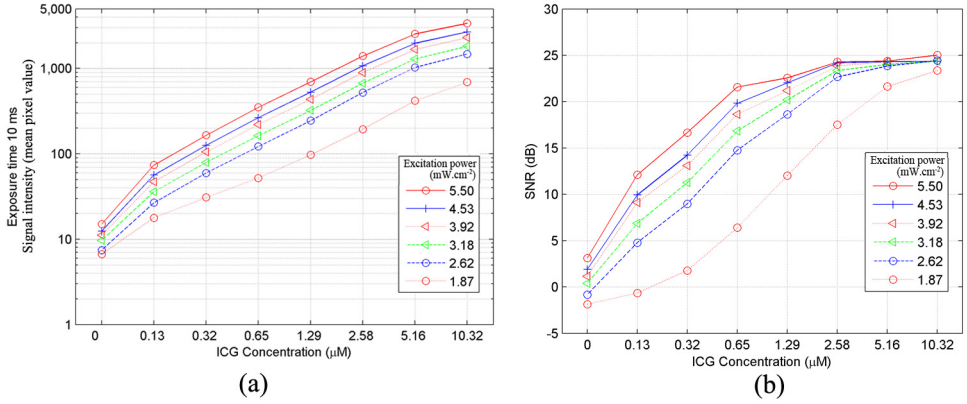

Fig. 6. (a) ICG sensitivity curve plot, showing the fluorescence signal intensity versus ICG concentration and NIR excitation power, and (b) SNR versus ICG concentration and NIR excitation power.

We also performed the fluorescence imaging experiment with chicken breast tissue to demonstrate the proposed method. The integration time of the camera was set to 10 ms and the ICG with a concentration of 25.8 μM was injected into chicken breast tissue. Figures 7(a) and 7(b) are the extracted color images when NIR excitation was off and on, Figs. 7(c) and 7(d) are images in the NIR channel when NIR excitation was off and on, respectively. The NIR fluorescence image, which is the difference between Figs. 7(c) and 7(d), is shown in Fig. 7(e). It is also displayed in false color shown in Fig. 7(f). The color image and the NIR fluorescence image are merged together and shown in Figs. 7(g) and 7(h) with different color maps and thresholds. From Figs. 7(e)-(h), the tissue texture and the fluorescence regions can be perceived clearly, demonstrating this system a powerful tool for image guided surgery under normal surgical lighting.

4. Conclusion

In this paper, we have demonstrated a single camera color and fluorescence image guided surgical system which can work under normal surgical light illumination. It consists of a RGB-NIR camera and synchronized NIR excitation illumination. Compared to other techniques, the proposed system is simple, compact, and low-cost; can capture color image and NIR fluorescence images in real time.

The proposed system extracts NIR fluorescence image from the NIR channels of the raw images captured with the surgical light and the room light, the bleed-through of the visible light into the NIR channel will impact the accuracy of fluorescence measurement. While we have already developed efficient algorithms to extract information from different channels, we will continue to improve the extract accuracy under the surgical lighting condition.

#212401 - $15.00 USD Received 20 May 2014; revised 17 Jul 2014; accepted 19 Jul 2014; published 25 Jul 2014

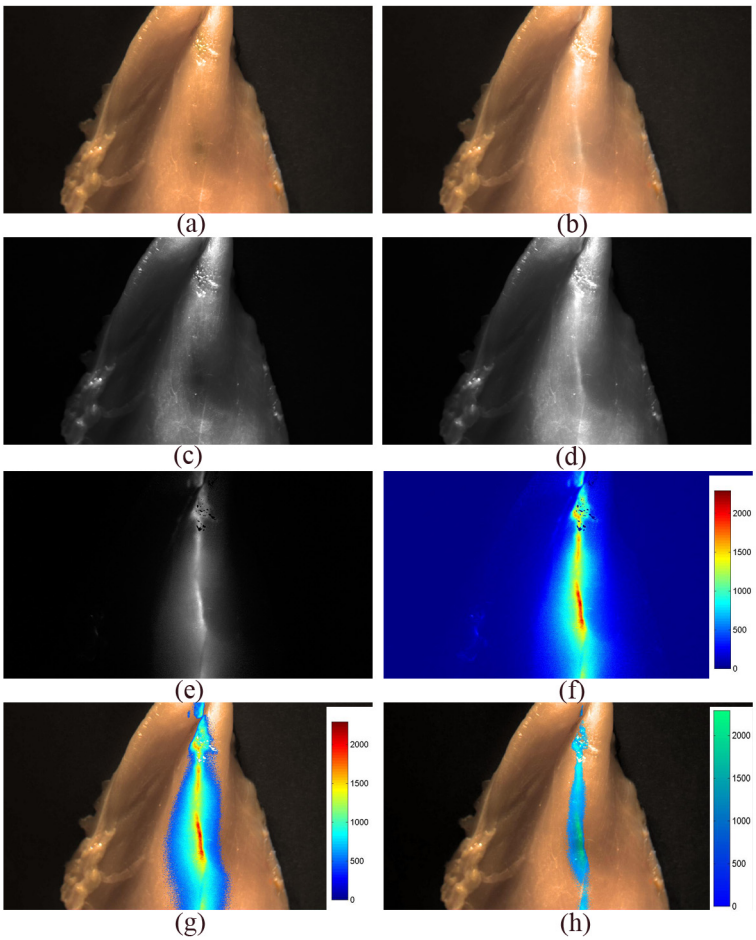

Fig. 7. (a) RGB image of chicken breast with excitation light off. (b) RGB image with excitation light on. (c) NIR image with excitation light off. (d) NIR image with excitation light on. (e) Difference image between (c) and (d). (f) Difference image displayed in false color. (g) Merged image of the difference image (f) and color image (a). (h) Merged image with different color map and threshold.

Acknowledgments

This work is partially supported by a grant of the China Scholarship Council.

#212401 - $15.00 USD Received 20 May 2014; revised 17 Jul 2014; accepted 19 Jul 2014; published 25 Jul 2014